

Low-temperature transition to a metallic state in $(\text{La}_{0.5}\text{Pr}_{0.5})_{0.7}\text{Ca}_{0.3}\text{MnO}_3$ films

N. A. Babushkina and L. M. Belova*

Institute of Molecular Physics, Russian Research Center "Kurchatov Institute," Kurchatov Square 1, Moscow, 123182 Russia

D. I. Khomskii

*Materials Science Center, University of Groningen, Nijenborgh 4, 9747 AG Groningen, The Netherlands
and Lebedev Physics Institute, Leninskii Prospect 53, Moscow, 117924 Russia*

K. I. Kugel

Scientific Center for Applied Problems in Electrodynamics, Izhorская Street 13/19, Moscow, 127412 Russia

O. Yu. Gorbenko and A. R. Kaul

Chemistry Department, Moscow State University, Vorobievsky Gory, Moscow, 119899 Russia

(Received 15 July 1998)

The electrical resistivity of epitaxial $(\text{La}_{0.5}\text{Pr}_{0.5})_{0.7}\text{Ca}_{0.3}\text{MnO}_3$ films deposited on single crystalline LaAlO_3 substrates was studied at temperature and magnetic fields ranging from 4.2 to 300 K and from 0 to 3 T, respectively. On cooling from room temperature at zero magnetic field, the films demonstrate at first the behavior typical of the charge-ordered (CO) insulating state, whereas below 40 K they undergo the transition to a metal-like state with slowly decreasing resistivity. On heating from 4.2 K, the films remain metallic and their resistivity $\rho(T)$ coincides with the cooling curve only at $T > 80$ K. This hysteretic behavior fully reproduces itself at repeated cooling-heating cycles. Near the low-temperature transition to a metal-like state the charge ordering (CO) is metastable and the resistivity exhibits the relaxation phenomena. The applied magnetic field as low as $H = 1$ T suppresses CO, and the temperature hysteresis gradually disappears. The $\rho(T)$ measurements at nonzero fields reveal a pronounced colossal magnetoresistance effect with the resistivity drop by a factor exceeding 10^6 at $H = 3$ T. It was also found that relatively small dc voltages (< 3 V) can cause the switching from CO to a metal-like state within the metastability range in the vicinity of 40 K when the charge ordering can be rather easily suppressed. Within this range, the current-voltage characteristics are highly nonlinear, with a memory effect: after switching the sample remains metallic even if the voltage is lowered. The observed effects are interpreted in terms of strong competition between charge ordering and ferromagnetic spin ordering. This competition can give rise to different kinds of spatial inhomogeneities involving the charge-ordered state, which should manifest themselves most clearly in the vicinity of the low-temperature transition to the metal-like state. The behavior of resistivity before the transition gives indications of the two-phase state. The transition itself can be a manifestation of a percolative nature of conductivity in this regime. [S0163-1829(99)06209-8]

I. INTRODUCTION

Magnetic oxides with metallic conductivity, especially those characterized by the colossal magnetoresistance (CMR) exhibit a whole wealth of interrelated phenomena such as metal-insulator transitions, orbital (or Jahn-Teller) ordering, charge ordering, double exchange, lattice and magnetic polarons, etc. (see, e.g., Ref. 1). This interplay provides a better insight into the origin of magnetism, the nature of electronic states, and transport phenomena in these materials. The compounds where the transition points corresponding to different types of ordering are close to each other are of special interest because small composition changes and relatively weak applied fields can produce rather pronounced effects.

A good example of such materials is presented by the doped rare-earth manganites $(\text{La}_{1-y}\text{R}_y)_{1-x}\text{A}_x\text{MnO}_3$ ($\text{R} = \text{Pr}, \text{Nd}$; $\text{A} = \text{Ca}, \text{Sr}$). These manganites are very sensitive to composition variations and can be switched, for example, from the insulator to the metallic state under effect of pres-

sure, magnetic and electric fields, and even x-ray irradiation.²⁻⁴ A dramatic manifestation of these phenomena is the metal-insulator transition induced by $^{16}\text{O} \rightarrow ^{18}\text{O}$ isotope substitution.⁵⁻⁷

The unusual behavior of these manganites stems from the strong competition between two possible types of states: a charge-ordered (CO) state where Mn^{3+} and Mn^{4+} are localized at separate sublattices (this state is insulating and usually antiferromagnetic) and a charge-delocalized (CD) ferromagnetic state with a metal-like conductivity. Note that Mn^{3+} is the Jahn-Teller ion, and the corresponding distortions of MnO_6 octahedra can give rise to the orbital ordering and to the additional stabilization of the CO state.

Above a certain characteristic temperature both CO and CD states transform to a charge-localized (CL) paramagnetic phase. The CD-CL transformation is accompanied by a significant increase in the electrical resistivity, and it is rather sensitive to the applied magnetic field giving rise to the CMR. For the CL state, it is usually assumed that charge carriers are polarons localized due to lattice distortions of the

Jahn-Teller (JT) type. This assumption was confirmed by various experimental techniques (see Ref. 8, and references therein). In several papers it was also demonstrated that ferromagnetic clusters exist well beyond the conventional fluctuation regime and can be interpreted as magnetic polarons.^{9,10} The lattice polaron model and magnetic polaron model can be reconciled under the assumption that the lattice polarons (associated with the fluctuating JT distorted regions) break the long-range ferromagnetic order leaving small ferromagnetic clusters, where the lattice is relatively undistorted.¹¹ The possibility of an inhomogeneous state was also considered in the case of CL-CO transformation. It was shown, for example, that the behavior of $\text{Nd}_{0.25}\text{La}_{0.25}\text{Ca}_{0.5}\text{MnO}_3$ is well interpreted in terms of the so-called incipient CO state without the fully developed long-range order.¹² This “soft” CO state can undergo a transition to the CD ferromagnetic phase at the lowering of temperature, even at zero magnetic field.^{7,12} For the usual CO state such a reentrant transition was observed only at relatively high magnetic fields.¹³

The studies of thin-film samples add complexity to this quite sophisticated picture. The substrate-induced strains can significantly shift the phase equilibria and introduce additional inhomogeneities (see, e.g., Ref. 14).

In this paper, we investigate the transport properties of $(\text{La}_{0.5}\text{Pr}_{0.5})_{0.7}\text{Ca}_{0.3}\text{MnO}_3$ thin films on LaAlO_3 substrates and show that these films are characterized the low-temperature transition from CO to ferromagnetic charge-delocalized state. Owing to the difference in composition and to the influence of strains induced by the substrate, the phase transition line becomes shifted in such a way that similar transition occurs even without the applied field.

The films of the composition $(\text{La}_{0.5}\text{Pr}_{0.5})_{0.7}\text{Ca}_{0.3}\text{MnO}_3$ exhibit in the most concentrated form a variety of unusual features characteristic of $(\text{La}_{1-y}\text{Pr}_y)_{0.7}\text{Ca}_{0.3}\text{MnO}_3$ family of compounds. The endmembers of this family $\text{La}_{0.7}\text{Ca}_{0.3}\text{MnO}_3$ and $\text{Pr}_{0.7}\text{Ca}_{0.3}\text{MnO}_3$ have the ferromagnetic metal and antiferromagnetic CO ground states, respectively. In bulk samples, the crossover between these two regimes occurs at $y=0.75$.¹⁵ The lattice constant of LaAlO_3 is smaller than that for manganites. The resulting in-plane contraction of the thin-film sample shifts the crossover toward smaller y values. Thus, at $y=0.5$ the bulk samples demonstrate the ferromagnetic metal-like behavior below the Curie point, whereas clear manifestations of CO are observed for the thin films in the same temperature range.

The high-resistance CO state is rather unstable and apparently inhomogeneous. It is strongly affected not only by moderate magnetic fields (about 0.2 T) but also (which should be specially emphasized) by relatively low voltages: the current-voltage characteristics in this regime are highly nonlinear, and the resistivity drops significantly (by a factor of 10^3-10^4) at voltages exceeding 3 V. All transformations in these thin films are characterized by strong hysteresis both in temperature and magnetic-field dependence of the resistivity. This striking behavior, in our opinion, is a signature of inhomogeneous nature of this state with the percolation-type conductivity (see, e.g., Ref. 16). As it is known, in manganites we often see the tendency to phase separation and formation of inhomogeneous states.^{7,12,17} Apparently we are dealing here with a similar situation. A strong decrease of

resistivity with magnetic field in a “metallic” phase may be explained in this picture. Even more conclusive are the data to be discussed below, about strongly nonlinear I - V characteristics of our samples in the vicinity of the transition from the highly resistive CO state to the low-temperature conductive state.

II. EXPERIMENT

The thin-film samples were manufactured by the aerosol MOCVD technique. The organic solutions of volatile precursors were nebulized in the carrier gas flow and then evaporated.¹⁸ As the precursors, we used $A(\text{thd})_3$ ($A=\text{La}$, Pr , Mn) and $\text{Ca}(\text{thd})_2$ compounds where thd is 1,2,6,6-tetramethylheptane-3,5-dionate. The 300 nm thick films were deposited onto (001) LaAlO_3 single crystalline substrates at 750°C. The partial pressure of oxygen was 3 mbar (the total pressure was 6 mbar). The as-deposited samples were cooled down and then annealed for half an hour at the deposition temperature in oxygen at the atmospheric pressure to fix their oxygen content.

The x-ray diffraction [four-circle diffractometer, Siemens D5000 with secondary graphite monochromator ($\text{Cu } K\alpha$ radiation)] was used to determine the phase composition, orientation, and lattice constants of the prepared films. We measured $\theta-2\theta$ scans and rocking curves. The SEM images were recorded by CAMSCAN equipped with an EDAX system for quantitative analysis. The SNMS (sputtered neutrals mass spectrometry) depth profiling was carried out using INA-3 system. The SNMS demonstrated that uniformity of the film composition was maintained accurate to 1%.

The x-ray-diffraction patterns of the films were pseudocubic, but the determination of the full set of lattice parameters revealed the tetragonal distortion correlating with film-substrate mismatch characteristic of this film. The strains in the film correspond to its compression in the film-substrate plane.

The measurements of electrical resistivity were performed using $3\times 10\text{ mm}^2$ bars cut from the $10\times 10\text{ mm}^2$ samples. We employed two standard measurement schemes, four-probe and two-probe. The two-probe scheme turned out to be more convenient in the current measurement setup at low temperatures, when resistivity values exceeded $10^{10}\ \Omega$, since it allowed to stabilize the dc voltage at a sufficiently high level. In this setup the fixed value of dc voltage was not affected by the dramatic changes of resistivity at low temperatures.

III. RESULTS

The temperature dependence of resistivity for the $\text{La}_{0.35}\text{Pr}_{0.35}\text{Ca}_{0.3}\text{MnO}_3$ thin film on a LaAlO_3 substrate at different magnetic fields is shown in Fig. 1. The zero-field curve demonstrates that resistivity $\rho(T)$ behaves in quite a different way on cooling and on heating. This form of resistivity curves is strictly reproducible at repeated cooling-heating cycles. On cooling from the room temperature, the resistivity gradually grows attaining the maximum value at about 60 K. After that, the slope of the curve becomes much smaller and a plateau in $\rho(T)$ is observed. A slow decrease in ρ in the plateau region is suddenly interrupted by the steep resistivity drop at about 40 K. Within the 40–20 K range the

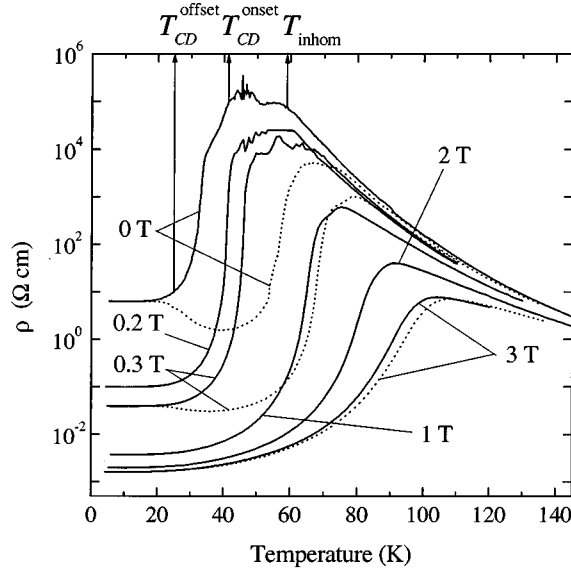


FIG. 1. Temperature dependence of the resistivity for a $(\text{La}_{0.5}\text{Pr}_{0.5})_{0.7}\text{Ca}_{0.3}\text{MnO}_3$ film at different values of the applied magnetic field. Solid lines indicate cooling curves, dotted lines indicate heating curves. T_{inhom} is the beginning of high-resistivity plateau corresponding to the two-phase region, $T_{\text{CD}}^{\text{onset}}$ and $T_{\text{CD}}^{\text{offset}}$ are temperatures corresponding to the beginning and the end of transition to the low-temperature metallic phase, respectively.

resistivity decreases by four orders of magnitude, then $\rho(T)$ flattens out and changes only slightly till 4.2 K. As a result, we observed a zero-field transition to a metal-like state at low temperatures.

On heating from 4.2 K, $\rho(T)$ first follows the cooling curve and then undergoes the further decrease by a factor of 1000 from 20 to 40 K. After that the resistivity grows again, passes through a peak with the flattened top, and finally coincides with the cooling curve at $T > 80$ K. Note that the high-resistivity plateau on heating is narrower than on cooling and shifted toward higher temperatures. The $\rho(T)$ behavior is characterized by the pronounced hysteresis typical of the first-order phase transition.

Near the low-temperature transition to the metal-like state the high-resistivity state is metastable. We tried to study in more detail the $\rho(T)$ behavior within this range with an emphasis on the relaxation phenomena. The results are illustrated in Fig. 2. We cooled the sample from 150 to 30 K and then fixed this temperature. After an hour of keeping the sample at 30 K the resistivity decreases to very low (metallic) value about 10 Ω cm. At subsequent heating up to 60 K and cooling down to 4.2 K, the $\rho(T)$ curve forms a flattened loop without changing its metal-like behavior. If we fix the temperature (on cooling) at 40 K, the similar drop in resistivity also occurs, but it takes more time (> 2 h) to attain the metal-like state. This shows that the high-resistivity state loses its stability at a certain temperature range above 20 K and the actual transition temperature depends on the cooling rate.

Figure 1 illustrates also the evolution of $\rho(T)$ curves at under the effect of applied magnetic field H ranging from 0.2 to 3 T. With the growth of H the peak in $\rho(T)$ becomes lower and shifts towards higher temperatures. At small magnetic fields ($H = 0.2$ and 0.3 T) the temperature hysteresis of

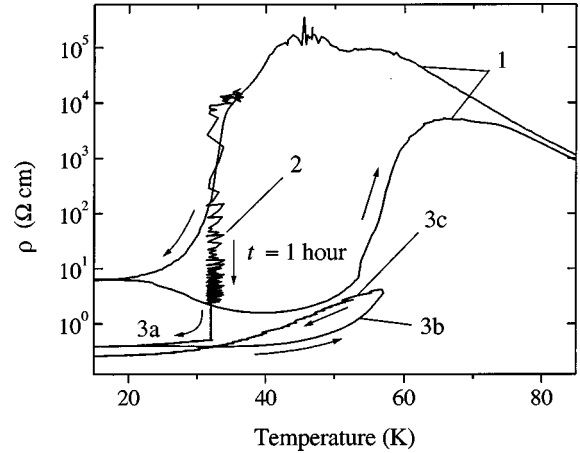


FIG. 2. Relaxation of the resistivity for the $(\text{La}_{0.5}\text{Pr}_{0.5})_{0.7}\text{Ca}_{0.3}\text{MnO}_3$ film near the transition to the low-temperature metallic phase: temperature dependence of the resistivity at zero magnetic field (curve 1); resistivity variations for the film kept for 1 h at fixed temperature $T = 30$ K (curve 2). Curve 3 illustrates the behavior of the sample in the low-resistivity state after the stage corresponding to curve 2: cooling from 30 to 4.2 K (curve 3a), heating up to 60 K (curve 3b), and cooling from 60 K to 4.2 K (curve 3c).

ρ still exists but the hysteresis loops become narrower than at $H = 0$. At $H > 1$ T, the $\rho(T)$ hysteresis gradually disappears giving clear indication to the suppression of the CO state. Note that usually the “melting” of CO state occurs at fields much higher than 1 T (characteristic value for PrCaMnO crystals is about 12 T).¹⁹ It is also of interest from the viewpoint of possible applications that a significant drop in resistivity occurs at very low fields (about 0.2–0.3 T). Note that resistivity in the low-temperature metal-like state also decreases with growth of the magnetic field (by more than three orders of magnitude at 3 T). Such a behavior gives a clear indication of the inhomogeneity of the metallic state. This point will be discussed in more detail in the next section.

The $\rho(T)$ measurements at nonzero fields revealed a clearly pronounced CMR, with the values being among the largest reported for manganites. The parameter characterizing magnetoresistance is chosen here as $\Delta = [\rho(H = 0) - \rho(3T)]/\rho(3T)$. Let us recall that for the system under study the applied magnetic field produces a double effect on the resistivity: first, the resistivity decreases near the Curie point T_C due to the reduction in electron scattering caused by the spin alignment, and second, the magnetic field suppresses charge ordering and stimulates the transition from the CO to the charge delocalized state. At the temperatures corresponding to the zero-field resistivity peak both mechanisms contribute to CMR and Δ is as high as 10^6 , whereas at low temperatures the magnetic field only helps to terminate the transition to the charge delocalized state already provoked by the temperature lowering and the corresponding Δ values are smaller (about 10^3).

The magnetic-field dependence of resistivity at two fixed temperatures 50 and 70 K is illustrated in Fig. 3. We see that magnetic field at 50 K induces the insulator-metal transition with the resistivity drop by several orders of magnitude. The $\rho(H)$ curves are hysteretic in the vicinity of this transition

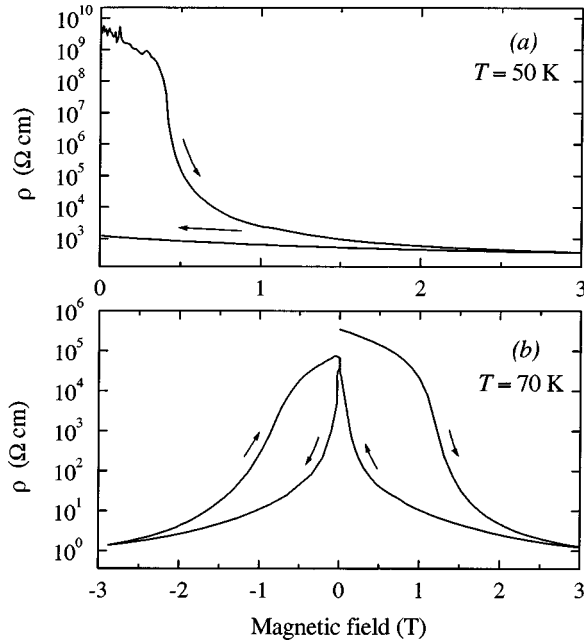


FIG. 3. Resistivity versus magnetic field at (a) $T = 50$ K and (b) $T = 70$ K. The field sweep direction is indicated by arrows.

magnetic field: if the field is decreased after the transition, the sample cannot even return to the high-resistance state (i.e., the charge delocalization became quenched, this is the case at $T = 50$ K). The hysteresis loop at 70 K is much narrower than at 50 K. The resistivity at 70 K decreases with the increasing field and then grows again when the field begins to decrease at the reverse run (according to the “melting” and “crystallization” of the CO state). These “melting” and “crystallization” occur at very low fields about 0.2 T. The zero-field resistance is reproduced after the field cycling but its value turns out to be lower than that for the virgin curve. Such lowering of the zero-field resistance can be attributed to a certain remanent spin ordering similar to that discussed for $\text{Pr}_{0.7}\text{Ca}_{0.3}\text{MnO}_3$.¹⁹

In addition to the CO suppression by magnetic field, we studied the electric-field effect on resistivity in the vicinity of low-temperature insulator–metal transition. The switching from insulating to metallic state induced by relatively high applied dc voltage was reported for $\text{Pr}_{0.7}\text{Ca}_{0.3}\text{MnO}_3$.³ For our samples, we expected that the behavior of resistivity will be also dependent on the applied voltage especially within the metastability range 40–60 K when the CO can be rather easily suppressed. The $\rho(T)$ curves (plotted both on cooling and heating) corresponding to different values of dc voltage applied across the sample are presented in Fig. 4. The measurements were performed using the standard two-probe scheme, which ensured maintaining the constant voltage and determining high values of resistivity (10^{10} Ω and higher) more accurately at currents as low as 0.01 nA. For each value of the applied voltage, we observe the hysteretic temperature dependence of ρ similar to that shown in Fig. 1.

At low voltages, the onset of the transition from the high-resistance CO state to the low-resistance charge delocalized state is preceded the plateau in resistivity. The plateau becomes narrower at higher voltages and eventually disappears. At small voltage $V = 1.3$ V, the transition is quite smooth and the resistivity value at 4.2 K is only by two

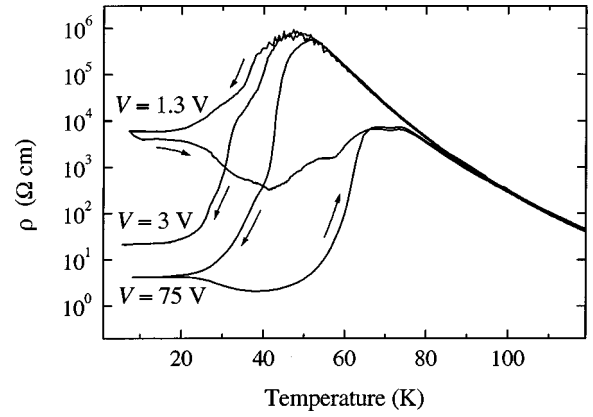


FIG. 4. Temperature dependence of the resistivity for a $(\text{La}_{0.5}\text{Pr}_{0.5})_{0.7}\text{Ca}_{0.3}\text{MnO}_3$ film at different values of applied dc voltage. The direction of the temperature change (cooling or heating) is indicated by arrows.

orders of magnitude lower than the initial value ρ_{onset} . However, at higher voltages from 3 to 75 V the resistivity decreases steeply and $\rho(4.2$ K) is lower than ρ_{onset} by a factor of the order 10^6 . The corresponding $\rho(T)$ curves on heating illustrate the features of the reverse transition to the high-resistance state. For $V = 3$ V, the $\rho(T)$ behavior upon heating is similar to that shown in Fig. 1. At higher voltages (e.g., at 75 V), the sample remains metal-like up to about 40 K and then transforms steeply to the high-resistance state. On heating, the peak values of ρ are nearly the same for different voltages, and the transition to the high-resistance state occurs within the same temperature range 65–80 K. Above 80 K, all $\rho(T)$ curves measured both on cooling and heating coincide.

Thus, at relatively low voltages (about 100 times lower than those reported in Ref. 3) we observed the switching from the CO to metal-like state accompanied by the pronounced hysteresis. The situation here is similar to the suppression of CO by magnetic field with very low characteristic field values. Both these effects are indicative of the low stability of CO. Note, that the sensitivity of the resistance to low dc voltages can be even more important for potential applications than the sensitivity to low magnetic fields.

To make the above picture more clear, we studied the relaxation of ρ under the effect of applied voltage and the current-voltage characteristics at different temperatures near the transition to metal-like state. The results are presented in Figs. 5 and 6, respectively. At 50 K, the resistivity remains nearly constant at sweeping the voltage from zero to 75 V and in the backward direction, whereas at 40 K ρ gradually decreases by a factor of 10^4 after several voltage sweeping cycles. The I - V curves are linear at 50 K, but at 40 K they exhibit a pronounced nonlinearity: dV/dI drops down by a factor of ten at small voltages (up to 3 V) then gradually decreases by four orders of magnitude up to 75 V. The sample transforms to the metal-like state and remains in it when the voltage is lowered. The metal-like state turns out to be “quenched,” the sample can be taken out from this state only by heating up to 150 K.

IV. DISCUSSION

The characteristic feature of the system under study is the existence of metal-like phase (presumably ferromagnetic) at

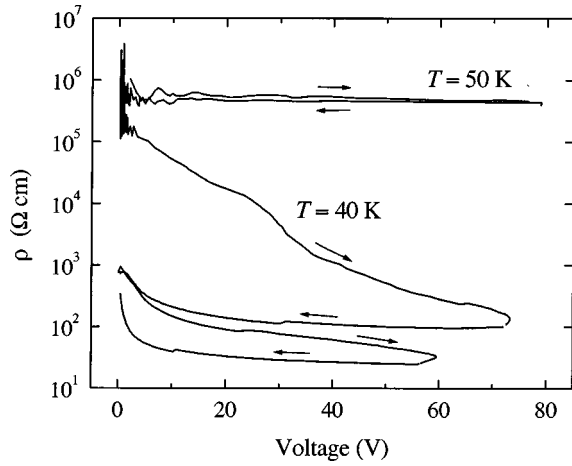


FIG. 5. Resistivity versus applied dc voltage at $T=50$ K and $T=40$ K. The voltage sweep direction is indicated by arrows.

zero magnetic field within the temperature range below charge ordering (CO) region. The possibility of such a situation can be illustrated by simple qualitative reasoning. In fact, the CO usually observed in manganites corresponds to two nearly equivalent sublattices formed by Mn^{3+} and Mn^{4+} ions. At half-filling (Ca content $x=0.5$) this configuration is the most favorable one, whereas at $x<0.5$ the “excess” electrons should be distributed somehow over the sublattices. This extra disorder can exist in the form of random distribution of these excess electrons (Mn^{3+} ions) in the checkerboard arrangement of Mn^{3+} and Mn^{4+} , typical for $x=0.5$, or in the form of random clusters, presumably metallic, with extra electrons immersed in regular checkerboard CO state. In both cases an additional configurational contribution S_0 to the entropy of CO state arises. In general, the low-temperature entropy of the CO state can be written as

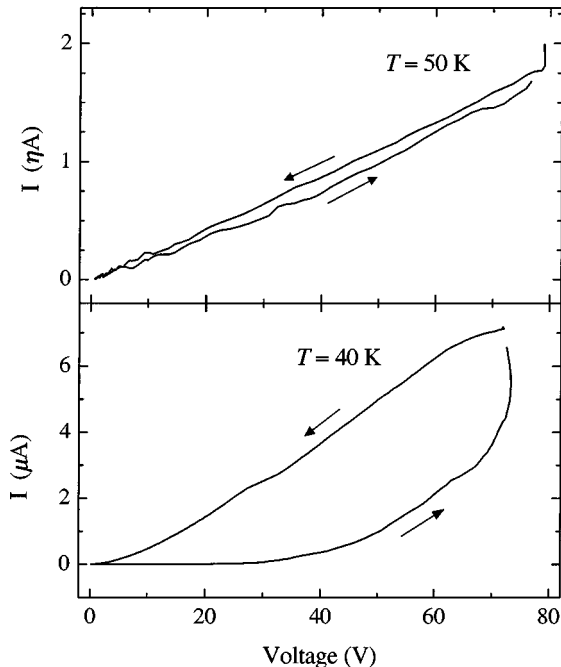


FIG. 6. Current-voltage characteristics for a $(\text{La}_{0.5}\text{Pr}_{0.5})_{0.7}\text{Ca}_{0.3}\text{MnO}_3$ film (a) at $T=50$ K (linear I - V curve) and (b) at $T=40$ K (nonlinear I - V curve).

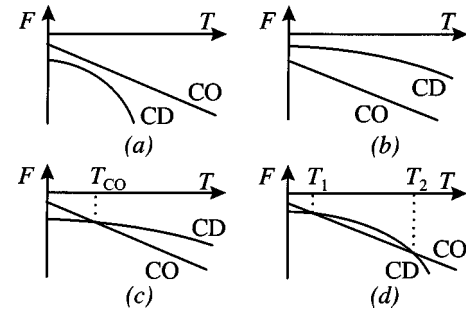


FIG. 7. Possible types of temperature dependence of the free energy in systems with competing insulating charge-ordered (CO) and metallic charge-delocalized (CD) states (the states with lower free energy come into play): (a) the system is metallic in the whole temperature range, (b) charge ordering in the whole temperature range, (c) the system is metallic below T_{CO} and charge ordered above T_{CO} , and (d) charge ordering within the limited temperature range ($T_1 < T < T_2$).

$$S_{\text{CO}} = S_0 + A \exp(-\Delta/T) + \tilde{\gamma}T, \quad (1)$$

where Δ is the band gap in the spectrum of the ordered charge carriers and $\tilde{\gamma}$ is the density of states of the quasifree carriers, which can exist in our system. On the other hand, the entropy of metallic state has a conventional form

$$S_M = \gamma T. \quad (2)$$

Note that in the case when the metal is ferromagnetic and the ferromagnetism is related to the double-exchange mechanism, the electron density of states γ at the Fermi level depends critically on the magnetization (the effective bandwidth increases with the ferromagnetic order parameter).

Turning now from entropy to the free energy $F = E - TS$, let us consider different types of low-temperature behavior of the system, which are schematically shown in Fig. 7. Cases (a) and (b) correspond to the metal-like CD and insulator-like CO states, respectively, in the entire temperature range. In the case (c), the low-temperature CD state gives way to the partially disordered CO state at increasing T . In case (d), CO exists within a limited temperature range. The low-temperature transitions from CO to the metallic state in cases (c) and (d) can be referred to as reentrant transitions since the possibility of metallic behavior lost at intermediate temperatures returns with the decreasing temperature. The ferromagnetic ordering in the metallic phase makes the latter situation even more probable since the growing order parameter gives rise to an additional decrease in the free energy of a metallic phase at low temperatures. Apparently, case (c) corresponds to the system under study, however the actual situation can be more complicated due to the possibility of spatially inhomogeneous states involving both charge-ordered and charge-delocalized regions.

Let us discuss in more detail the possible inhomogeneities for composition under study. The analysis of $d \ln \rho/d(1/T)$ curves shows that there is only a slight feature at $T=200$ K that can hardly be attributed to the onset of the fully developed CO ordering, but the steep growth of resistance below this temperature is quite typical of the CO state. On the other hand, the neutron-diffraction studies for powders of the same composition which exhibit clearly pro-

nounced ferromagnetism at low temperatures, reveal the enhanced lattice distortions between 200 K and the Curie point $T_C = 170$ K.²⁰ This gives certain indications to the existence of another state below 200 K characterized by local lattice distortions which can be related to a short-range (at least) orbital and charge order. Such a state bears clear similarities to the incipient CO state discussed in (Ref. 12). At decreasing T , we observed a plateau in the $\rho(T)$ curves. This plateau provides an evidence that some low-resistance regions appear within the CO background and we have, in fact, the two-phase state with metallic inclusions. This state becomes unstable at $T < 50$ K and eventually undergoes a first-order transition to the ferromagnetic charge delocalized state, which can also be characterized by phase segregation (as in Ref. 7). This transition is characterized by a very broad hysteresis, and metallic conductivity retains on heating until the transition to the CL paramagnetic state.

Thus, the inhomogeneous state involving charge ordering can be more favorable than pure CO below 200 K when CL paramagnetic phase becomes unstable. This “incipient CO” has higher configurational entropy which broadens the range of its stability toward higher temperatures. The nonuniform strains in our epitaxial film also favor the phase inhomogeneity and even phase separation. Such an inhomogeneous state seems also to be preferable from the viewpoint of optimum charge distribution since it is more natural to form the regions with the most stable CO corresponding to half-filling (one charge carrier per two Mn sites, $\text{Mn}^{3+}:\text{Mn}^{4+} = 1:1$) with the excess charge carriers distributed outside them. The CO regions can persist even below the low-temperature transition giving rise to relatively high resistivity of the metal-like state at low temperatures observed in our experiments (see the zero-field curve in Fig. 1). The applied magnetic field, electric field, or heating favors the “melting” of CO clusters embedded in the metallic phase causing an additional decrease in resistivity. The lowest resistivity observed in the metallic state corresponds to the full melting of CO clusters (see Figs. 1, 2 and 4).

In this picture, the low-temperature transition itself can be related to the onset of percolation through the metal-like CD regions. In the vicinity of the transition, the CO state is metastable and the actual transition point depends on the cooling rate. The applied magnetic field or pressure provides the spin alignment favoring the growth of metallic regions at the expense of charge-ordered ones. A similar effect is produced by the electric field which stretches the CO regions lowering their stability. This causes the growth of metallic inclusions within the CO host preferably along the electric field. When the CO regions are within the metastability range or close to it, the electric field readily melts them causing the merging of oriented metallic droplets. Such a percolationlike picture can give rise to the observed nonlinearity of I - V curves or even to the switching to the metallic state corresponding to the percolation threshold.

Our experimental results and the above discussion allow us to draw a schematic phase diagram in the T - H plane shown in Fig. 8. In this phase diagram, the characteristic temperatures and magnetic fields are determined from $\rho(T)$ curves for several fixed values of magnetic field (Figs. 1 and 2) and from $\rho(H)$ curves at different temperatures (Fig. 3). The high-resistance plateau between T_{inhom} and $T_{\text{CD}}^{\text{onset}}$ in Fig.

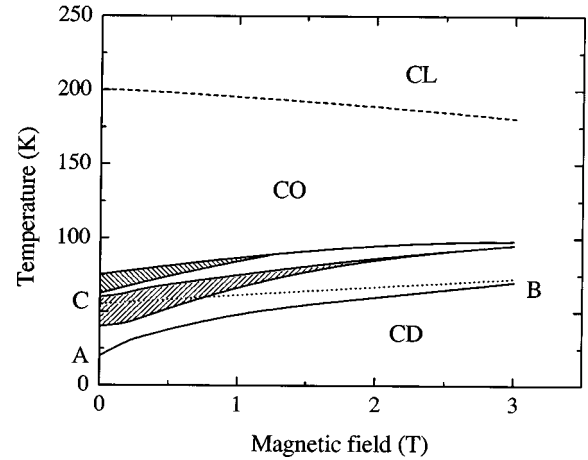


FIG. 8. Phase diagram in H - T coordinates for the $(\text{La}_{0.5}\text{Pr}_{0.5})_{0.7}\text{Ca}_{0.3}\text{MnO}_3$ film. The hatched areas correspond to the plateau regions in Fig. 1, i.e., to the two-phase state (CO with metallic inclusions). The hatches with positive and negative slope correspond to cooling and heating, respectively. The metallic phase on cooling is below the AB line, whereas on heating it exists below the CB line.

1 (hatched region in the phase diagram) is interpreted as the region of the inhomogeneous (maybe two-phase) state. The low-temperature boundary of the hatched area is not stable and depends on the cooling rate. Below the AB curve (corresponding to $T_{\text{CD}}^{\text{offset}}$ in Fig. 1) the behavior of resistivity is metal-like, though the metallic state can also be phase segregated. The low-temperature transition to the metallic state exhibits a pronounced hysteresis, therefore the boundaries of the metal-like state are different on cooling and on heating (AB and CB, respectively). The corresponding plateau regions are marked by hatches with positive and negative slope in Fig. 8. The hysteretic region is rather wide reflecting the enhanced stability of the inhomogeneous two-phase state. The boundary between the high-temperature charge-localized state and the CO state is shown by a dashed line since it is quite difficult to find out the exact temperature of this transition due to the possibility of the incipient character of charge ordering.

V. CONCLUSIONS

The mixed manganites $(\text{La}_{1-y}\text{Pr}_y)_{0.7}\text{Ca}_{0.3}\text{MnO}_3$ exhibit a large diversity of properties. For the films $(\text{La}_{0.5}\text{Pr}_{0.5})_{0.7}\text{Ca}_{0.3}\text{MnO}_3$ on a LaAlO_3 substrate we observed the low-temperature transition from the charge ordered to metallic state at decreasing temperature. The resistivity of these films is characterized by the remarkable sensitivity to variations of applied magnetic field and dc voltage, as well as by the clearly pronounced hysteresis with respect to both magnetic field and temperature. All these features are apparently related to the strong competition between charge ordering and ferromagnetism, which can result in spatially inhomogeneous CO state within a wide temperature and magnetic-field range. Such an inhomogeneity seems to be responsible for the unusual behavior of resistivity in the vicinity of the low-temperature transition to the metallic state. The specific type of the inhomogeneous state is still not clear

and the further, especially structural, studies are needed. However, the recent publications suggest the possibility of an “incipient” CO state with a not fully developed long-range charge-ordered,¹² phase-segregated state,⁷ or alternating charge-ordered and charge-delocalized stripes.²¹ The stripe structure seems to be quite probable in the temperature range of high-resistance plateau above the transition to the metallic state. In addition to its purely scientific interest, such a large sensitivity of these films to relatively small external fields (change of resistivity by a factor of 10^4 – 10^5 in magnetic field about 0.2–0.3 T and at voltages about 3 V) opens up fresh opportunities for applications.

ACKNOWLEDGMENTS

The authors are grateful to A. N. Taldenkov, A. V. Inyuskin, and E. A. Chistotina for their helpful assistance at different stages of this work. The work is partially supported by the Russian Foundation for Basic Research (Projects No. 97-03-32979a and 96-15-96738) and by INTAS (Grant No. 97-0963). D. I. Khomskii acknowledges the support of the Netherlands Foundation for the Fundamental Study of Matter (FOM) and of the European Union through the OXSEN program.

*Electronic address: belova@imp.kiae.ru

¹D. I. Khomskii and G. A. Sawatzky, *Solid State Commun.* **102**, 87 (1997).

²A. Asamitsu, Y. Moritano, Y. Tomioka, T. Arima, and Y. Tokura, *Nature (London)* **373**, 407 (1995).

³A. Asamitsu, Y. Tomioka, H. Kuwahara, and Y. Tokura, *Nature (London)* **388**, 50 (1997).

⁴V. Kiryukhin, D. Kasa, J. P. Hill, B. Keimer, A. Vigliante, Y. Tomioka, and Y. Tokura, *Nature (London)* **386**, 813 (1997).

⁵G.-M. Zhao, K. Conder, H. Keller, and K. A. Müller, *Solid State Commun.* **104**, 57 (1997).

⁶N. A. Babushkina, L. M. Belova, O. Yu. Gorbenko, A. R. Kaul, A. A. Bosak, V. I. Ozhogin, and K. I. Kugel, *Nature (London)* **391**, 159 (1998); N. A. Babushkina, L. M. Belova, V. I. Ozhogin, O. Yu. Gorbenko, A. R. Kaul, A. A. Bosak, D. I. Khomskii, and K. I. Kugel, *J. Appl. Phys.* **83**, 7369 (1998).

⁷M. R. Ibarra, G.-M. Zhao, J. M. De Teresa, B. Garcia-Landa, Z. Arnold, C. Marquina, P. A. Algarabel, H. Keller, and C. Ritter, *Phys. Rev. B* **57**, 7446 (1998).

⁸A. P. Ramirez, *J. Phys.: Condens. Matter* **9**, 8171 (1997).

⁹J. W. Lynn, R. W. Erwin, J. A. Borchers, Q. Huang, A. Santoro, J.-L. Peng, and Z. Y. Li, *Phys. Rev. Lett.* **76**, 4046 (1996).

¹⁰J. M. De Teresa, M. R. Ibarra, P. A. Algarabel, C. Ritter, C. Marquina, J. Garcia, A. del Moral, and Z. Arnold, *Nature (London)* **386**, 256 (1997).

¹¹D. E. Cox, P. G. Radaelli, M. Maresio, and S.-W. Cheong, *Phys. Rev. B* **57**, 3305 (1998).

¹²A. Arulraj, A. Biswas, A. K. Raychaudhuri, C. N. R. Rao, P. M. Woodward, T. Vogt, D. E. Cox, and A. K. Cheetham, *Phys. Rev. B* **57**, R8115 (1998).

¹³Y. Tomioka, A. Asamitsu, H. Kuwahara, and Y. Tokura, *J. Phys. Soc. Jpn.* **66**, 302 (1997).

¹⁴A. J. Millis, T. Darling, and A. Migliori, *J. Appl. Phys.* **83**, 1588 (1998).

¹⁵H. Y. Hwang, S.-W. Cheong, P. G. Radaelli, M. Marezio, and B. Batlogg, *Phys. Rev. Lett.* **75**, 914 (1996).

¹⁶L. P. Gor'kov and V. Z. Kresin, *Pis'ma Zh. Eksp. Teor. Fiz.* **67**, 934 (1998).

¹⁷M. Yu. Kagan, D. I. Khomskii, and M. Mostovoy, cond-mat/9804213 (unpublished).

¹⁸O. Yu. Gorbenko, A. R. Kaul, N. A. Babushkina, and L. M. Belova, *J. Mater. Chem.* **4**, 1585 (1994).

¹⁹H. Yoshizawa, H. Kawano, Y. Tomioka, and Y. Tokura, *J. Phys. Soc. Jpn.* **65**, 1043 (1996).

²⁰A. M. Balagurov, V. Yu. Pomyakushin, V. L. Aksenov, N. A. Babushkina, L. M. Belova, O. Yu. Gorbenko, A. R. Kaul, N. M. Plakida, P. Fisher, M. Gutman, and L. Keller, *Pis'ma Zh. Eksp. Teor. Fiz.* **67**, 672 (1998).

²¹S. Mori, C. H. Chen, and S.-W. Cheong, *Nature (London)* **392**, 473 (1998).